Periodica Polytechnica
Civil Engineering

62(1), pp. 33–47, 2018
https://doi.org/10.3311/PPci.10635

RESEARCH ARTICLE

Inelastic Displacement Ratios for Evaluation of Degrading Peak – Oriented SDOF Systems

Muzaffer Borekci[1*], Murat S. Kirçil[1], Ibrahim Ekiz[2]

Received 15 February 2017; Revised 25 April 2017; Accepted 12 May 2017

Abstract

Estimation of the inelastic displacement demand (IDD) is an important part of the performance-based design. Coefficient method is one of the methods for the estimation of IDD and in this method, IDD is determined by multiplying elastic displacement demand with inelastic displacement ratio (C_R). Previous researches showed that structures deteriorate and also exhibit dynamic instability under severe earthquakes and these behaviors should be considered in the estimation of C_R to estimate a reliable IDD. In this study, C_R of the non-degrading bilinear hysteretic model and the degrading peak-oriented hysteretic model with collapse potential were determined and effects of degradation on IDD were investigated. Nonlinear time history analysis of SDOF systems were performed using considered hysteretic models. Furthermore a new equation is proposed for the mean C_R of degrading SDOF systems. Also, effect of local site conditions and post-yield stiffness on the mean C_R of degrading SDOF systems were investigated.

Keywords

inelastic displacement ratio, nonlinear response, degradation, dynamic instability, collapse

[1]Department of Civil Engineering
Yildiz Technical University,
Istanbul, Turkey
[2]Department of Civil Engineering,
Faculty of Engineering,
Fatih Sultan Mehmet University,
Istanbul, Turkey
[*]Corresponding author email: mborekci@inm.yildiz.edu.tr

1 Introduction

Displacement-based design is used rather than forced-based design for the evaluation and/or design of structures. Structures are expected to behave nonlinearly under the effect of severe earthquakes and may suffer heavy damage because of the large lateral displacement demand. Thus, estimation of the inelastic displacement demand of structures is an important issue in performance-based design. Although, nonlinear time history analysis of structures is a more realistic method and may produce a better estimation of inelastic displacement demand of a structure, it is still not practical for engineering practice. Reliable and simpler methods are still required for the estimation of lateral inelastic displacement demand of structures.

Many researchers proposed several methods for the estimation of the lateral inelastic displacement demand of structures based on the relationship between elastic and inelastic displacement demand. They generally estimated inelastic displacement demand to elastic displacement demand ratio so-called "*inelastic displacement ratio*". The first study about the relationship between the inelastic and elastic displacement demand was made by Veletsos and Newmark in [1]. They investigated the relationship between the elastic and inelastic displacement demand of *single degree of freedom* (SDOF) systems using three earthquake ground motions, based on the elastic-perfectly plastic behaviour. They observed that deformation of elastic and inelastic systems are very close for SDOF systems with long periods and this observation gave well-known "*equal displacement rule*". Also they concluded that inelastic deformation demand is significantly higher than the elastic deformation demand for SDOF systems with short periods. Newmark and Hall proposed equations in [2] to obtain the inelastic response spectrum by using elastic response spectrum.

Shimazaki and Sozen [3] studied on the displacement demand of elastic and inelastic systems based on 5 different hysteretic models (Bilinear and Clough models) using El-Centro record. They concluded that elastic and inelastic displacement demands are very close for the periods longer than the transition period (characteristic period) between the constant acceleration and the constant velocity regions confirming the "equal displacement rule" independently of hysteretic models. Also they concluded that inelastic displacement demand of a system is higher than the displacement demand of the corresponding elastic system with period shorter than the characteristic period. Furthermore they observed that the difference of inelastic and elastic displacement demand of a system changes with the hysteretic model and function of the lateral strength. Conclusions given by Shimazaki and Sozen [3] were confirmed by Qi and Moehle [4].

Miranda studied the inelastic displacement ratio for mean constant ductility using 124 ground motion records in [5], [6], [7] and gave some results for this ratio in the short period range and the limiting periods of the spectral regions where the equal displacement rule is applicable. Miranda [8] proposed an equation for the inelastic displacement ratio of SDOF systems with constant ductility using 264 ground motion records, recorded on firm sites, based on elastic-perfectly plastic hysteretic behavior. Ruiz-Garcia and Miranda [9] conducted a similar study with the aforementioned one and proposed an equation for the inelastic displacement ratio of SDOF systems with constant lateral strength. They considered 216 ground motion records and used elastic-perfectly plastic hysteretic system.

Nassar and Krawinkler [10], Rahnama and Krawinkler [11], Seneviratna and Krawinkler [12] also studied on the inelastic displacement demand. They used bilinear model and Clough model which considers the strength degradation, stiffness deterioration or pinching effect, separately. Nassar and Krawinkler proposed an equation in [10] for the ratio of inelastic to elastic spectral displacement for the bilinear hysteretic behavior with different post-yield stiffness values.

Structures deteriorate under repeated cyclic loading in the inelastic response range [22]. Many researchers studied experimentally on the response of reinforced concrete (RC) buildings or members under cyclic loading and showed that the hysteretic behavior does not match with bilinear model and stiffness and strength degradation occurs throughout cyclic loading [23]. Thus, stiffness and strength degradation with softening branch (negative stiffness) must be considered in the estimation of inelastic displacement ratio of SDOF systems so that the cyclic behavior of the structures can be taken into consideration realistically. Softening branch, also called post-capping branch, has negative slope and it occurs after reaching the maximum strength of the hysteretic cycle.

Using an energy-based degrading hysteretic model and considering the softening branch in hysteretic behavior for the estimation of inelastic displacement demand may be helpful to determine the collapse potential of the considered structures. Chintanapakdee and Jaiyong [24] showed that displacement time history of SDOF systems is very close to the roof displacement of the corresponding *multi degree of freedom (MDOF)* RC moment-resisting frames if a degrading peak-oriented hysteretic model is used instead of non-degrading bilinear hysteretic model. Most of the studies mentioned above did not taken the degradation effect into account and generally use bilinear hysteretic model. Furthermore, studies considered the degradation took stiffness or strength degradation into account separately and did not consider collapse potential. Although Chenouda and Ayoub [19] used an energy-based stiffness and strength degrading hysteretic model with collapse potential in their study, they considered limited number of degradation cases for the investigation of the degradation effect on inelastic displacement ratio.

As a summary, previous studies were generally considered simple non-degrading hysteretic behavior in the estimation of inelastic displacement ratio. However, as it is mentioned above all materials deteriorate under cyclic loadings and hysteretic behavior of RC buildings appears similar to peak-oriented hysteretic model. It is clear that RC buildings with same period and stiffness can have different ductility and strength levels. Those differences result different degradation cases and collapse potential in the seismic loadings. Using same bilinear hysteretic model for RC buildings which have same stiffness but different degradation cases and collapse potential is not proper. Some studies used degradation and peak-oriented model but they generally considered strength and stiffness degradation separately and did not considered collapse potential which is very important for seismic behavior of a structure under seismic loading. It is thought that using a stiffness and strength degrading peak-oriented hysteretic model with collapse potential in the estimation of inelastic displacement ratio gives more approximate results for real buildings behavior.

In this study, inelastic displacement ratios of SDOF systems were investigated using an energy-based stiffness and strength degrading peak-oriented hysteretic model with collapse potential. A new equation for the estimation of inelastic displacement ratio is also proposed as a function of strength reduction factor, period and degradation parameters. Effect of degradation parameters on inelastic displacement ratio is also investigated. Furthermore, inelastic displacement ratios obtained for degrading peak-oriented and non-degrading bilinear models are compared. In addition to above investigations, effect of local site conditions and post-yield stiffness on inelastic displacement ratio were investigated.

2 Hysteretic Models

2.1 Bilinear Hysteretic Model

A finite slope is assigned to the stiffness after yielding to simulate the strain hardening characteristics of the steel and the reinforced concrete [25]. The backbone curve of the bilinear model was shown in Fig. 1. In the figure, K_e is elastic (initial) stiffness, K_s is post-yield stiffness, α_s is post-yield stiffness ratio, f_y is yield strength and u_y is yield displacement. Backbone curve can be defined by using three parameters; K_e, K_s and f_y.

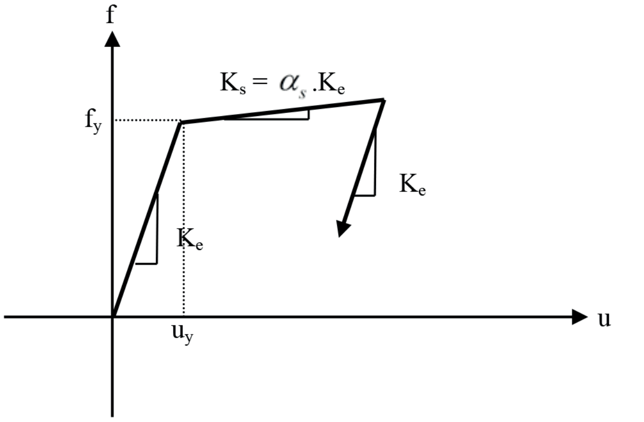

Fig. 1 Backbone curve of bilinear hysteretic behavior

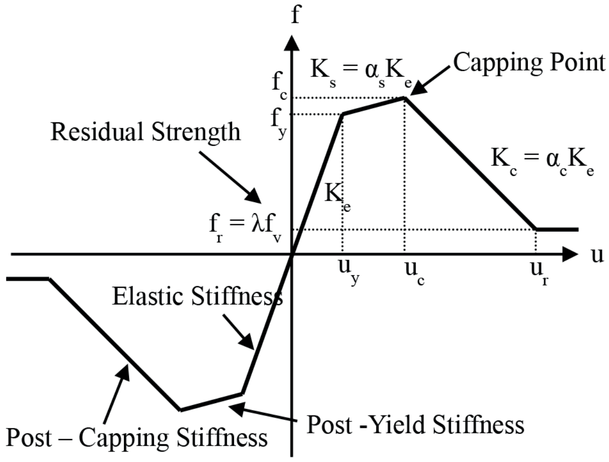

Fig. 2 Backbone curve of Peak-Oriented hysteretic behavior

2.2 Peak-Oriented Hysteretic Model

Experimental studies showed that the response of RC buildings or members under cyclic loading does not match with bilinear hysteretic behavior and stiffness and strength degradation occurs throughout the cyclic loading [23]. Degradation has significant effect on the deformation demand especially in the short period region of response spectrum. Thus, stiffness and strength degrading peak-oriented hysteretic model must be considered for the estimation of inelastic displacement ratio of SDOF systems so that the cyclic behavior of the existing building stock can be taken into consideration realistically. In this study, an energy-based stiffness and strength degrading peak-oriented hysteretic model with the collapse potential was considered.

This model keeps basic hysteretic rules proposed by Clough and Johnston in [26] and later modified by Mahin and Bertero in [27], but the backbone curve was modified by Ibarra et al. in [22] to include strength capping and residual strength as shown in the Fig. 2 [22].

In Fig. 2, f_r is the residual strength, f_c is the maximum strength, u_c is the displacement at which the beginning of softening branch which is called cap displacement and K_c is the post – capping stiffness which usually has a negative value. The basic idea of the model is that the reloading path always targets the previous maximum displacement.

Rahnama and Krawinkler [11] adopted a rule, which is defined below, in the Modified-Clough model to account for degradation effect. Four different deterioration modes can occur after the loading path reaches the yielding point at least in one direction. These deterioration modes are basic strength deterioration, post – capping deterioration, unloading stiffness degradation and reloading stiffness degradation. Description of the deterioration modes can be seen in Fig. 3.

The deterioration in excursion i is defined by a deterioration parameter β_i.

$$\beta_i = \left(\frac{E_i}{E_t - \sum_{j=1}^{i} E_j} \right)^c \tag{1}$$

E_i is the hysteretic energy dissipated in excursion i, E_t is the hysteretic energy dissipation capacity, ΣE_j is the hysteretic energy dissipated in all previous excursions and c is a component which defines the rate of deterioration. Reasonable range of c is between 1.0 and 2.0 [11]. The value of 2.0 slows down the rate of deterioration in early cycles and accelerates the rate of deterioration in later cycles, whereas a value of 1.0 implies an almost constant rate of deterioration. The hysteretic energy dissipation capacity is defined with Eq. (2).

$$E_t = \gamma f_y u_y \tag{2}$$

γ expresses the hysteretic energy dissipation capacity as a function of twice the elastic strain energy at yielding ($f_y u_y$). The parameter γ can have different values for each deterioration mode. Different indices are used for different deterioration modes; γ_s is for *basic strength deterioration*, γ_c is for *post-capping strength deterioration*, γ_u is for *unloading stiffness deterioration* and γ_a is for accelerated reloading stiffness deterioration. However using the same value of γ for all deterioration modes are sufficient for considering of the effect of cyclic deterioration [22]. Deterioration occurs with the combination of these four deterioration modes. Detailed information can be seen in the study of Ibarra et al. [22]

2.2.1 Degradation parameters

Ibarra et. al [22] suggested γ, u_c/u_y, α_c as the degradation parameters. Although the parameter *c* affects the cyclic deterioration, Ibarra et al. [22] concluded that a constant value of 1 for *c* is proper to investigate the effect of degradation on inelastic displacement ratios and this suggestion (*c* = 1) is followed in this study. All those deterioration parameters were calibrated for different material types by the experimental data [11].

γ indicates the rate of deterioration and deterioration rate gets slower with the increasing value of γ. γ = 50, γ = 100, γ = 150 and γ = Infinitive represent severe, moderate, low degradation and non-degrading systems, respectively [19]. Hysteretic behaviour becomes non-degrading for infinitive value of γ.

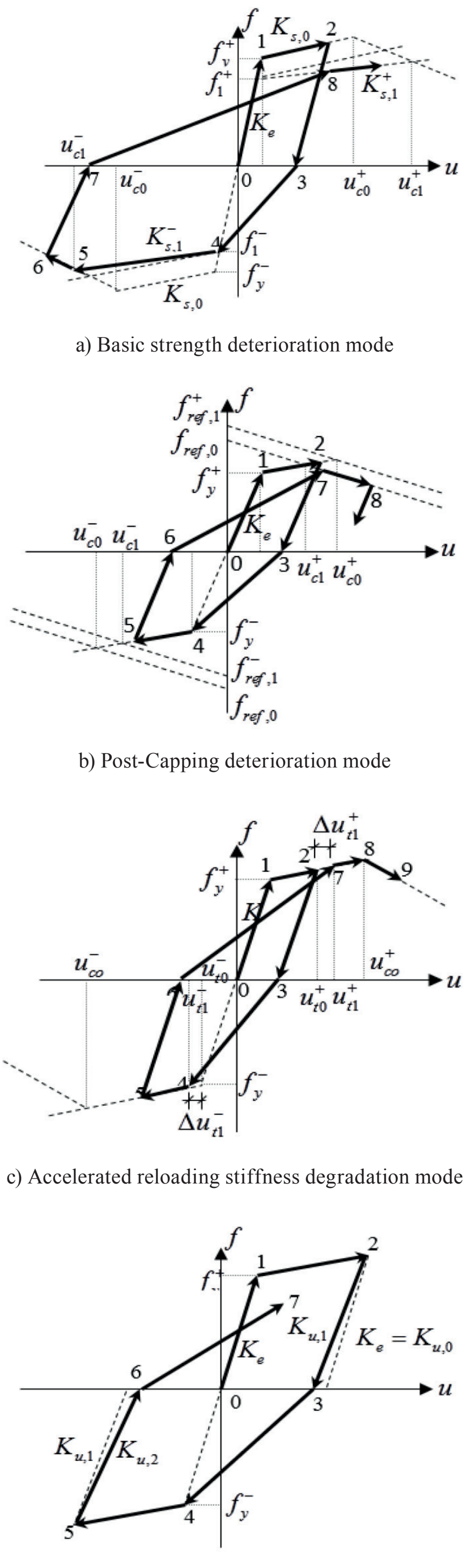

a) Basic strength deterioration mode

b) Post-Capping deterioration mode

c) Accelerated reloading stiffness degradation mode

d) Unloading degradation mode

Fig. 3 Basic strength and stiffness deterioration modes [22]

u_c/u_y is another degradation parameter and this ratio defines the beginning point of the negative slope of the hysteretic cycle. The strength degradation through the negative slope of the hysteretic cycle is defined as in-cycle degradation in FEMA 440 [28]. u_c/u_y is the ratio between corresponding displacement of peak and yield strength and u_c/u_y = 2, 4, 6 are used in this study. u_c/u_y = 2, 4, 6 represent non-ductile, medium ductile and very ductile structures, respectively [29].

α_c is used to define post-capping stiffness ratio and has negative values. The values of α_c are -6% [19], -14% and -21% [30] which represent small, medium and large slope, respectively. -14% is assumed as the medium slope in this study. Collapse potential is very sensitive to the change in small α_c values. However, if this parameter is very large the collapse potential is not greatly affected by variation of α_c [29]. Thus, larger values of α_c have not been considered in this study.

A parametric study was performed with 27 combinations of degradation parameters of considered hysteretic model. Combinations of deterioration parameters and the labelling of the combinations are given in Table 1.

Table 1 Considered combinations of deterioration parameters

Name	γ	α_c	u_c/u_y
γ50_α_c6_u_c/u_y2	50	-6%	2
γ50_α_c6_u_c/u_y4	50	-6%	4
γ50_α_c6_u_c/u_y6	50	-6%	6
γ50_α_c14_u_c/u_y2	50	-14%	2
γ50_α_c14_u_c/u_y4	50	-14%	4
γ50_α_c14_u_c/u_y6	50	-14%	6
γ50_α_c21_u_c/u_y2	50	-21%	2
γ50_α_c21_u_c/u_y4	50	-21%	4
γ50_α_c21_u_c/u_y6	50	-21%	6
γ100_α_c6_u_c/u_y2	100	-6%	2
γ100_α_c6_u_c/u_y4	100	-6%	4
γ100_α_c6_u_c/u_y6	100	-6%	6
γ100_α_c14_u_c/u_y2	100	-14%	2
γ100_α_c14_u_c/u_y4	100	-14%	4
γ100_α_c14_u_c/u_y6	100	-14%	6
γ100_α_c21_u_c/u_y2	100	-21%	2
γ100_α_c21_u_c/u_y4	100	-21%	4
γ100_α_c21_u_c/u_y6	100	-21%	6
γ150_α_c6_u_c/u_y2	150	-6%	2
γ150_α_c6_u_c/u_y4	150	-6%	4
γ150_α_c6_u_c/u_y6	150	-6%	6
γ150_α_c14_u_c/u_y2	150	-14%	2
γ150_α_c14_u_c/u_y4	150	-14%	4
γ150_α_c14_u_c/u_y6	150	-14%	6
γ150_α_c21_u_c/u_y2	150	-21%	2
γ150_α_c21_u_c/u_y4	150	-21%	4
γ150_α_c21_u_c/u_y6	150	-21%	6

Degradation has two components as cyclic and in-cycle whose details are defined in FEMA 440 [28]. The hysteretic model used in this study considers both aforementioned components of degradation. Cyclic and in-cycle components of degradation are shown in Fig. 4. From now on, all the degradation terms represents both cyclic and in-cycle effects.

3 Dynamic Instability

The structure subjected to a certain input is stable if small increase in the magnitude of the excitation result in small changes in the response [31]. Otherwise, structure will not be stable and it is called dynamic instability. Same assumption is also made by Villaverde [32]. In this study when the post-capping branch intersects the horizontal axis it is assumed that dynamic instability occurs and the *system collapses* [19], [22], [30], [33]. An illustration can be seen in Fig. 4.

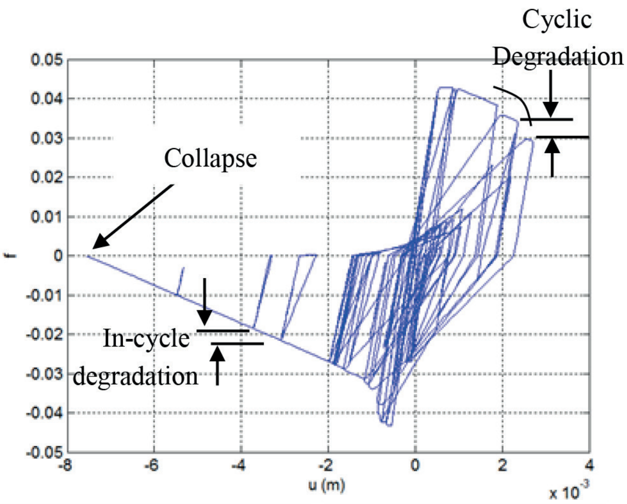

Fig. 4 An example for a hysteretic behavior with cyclic degradation and collapse

4 Ground Motion Records

A total of 160 earthquake acceleration time histories were used in this study. 80 records were considered with two horizontal components at each station and magnitude of the records ranges from 6 to 7.9. The earthquake acceleration time histories were divided into four groups according to local soil conditions at the recording station. Each group consisted of 40 ground motions. Locations of stations in the first group correspond to site class A, second group corresponds to site class B, third group corresponds to site class C and the last group corresponds to site class D according to USGS classification [34]. The average shear wave velocity of the first group is higher than 750 m/s. The second group consists of ground motions with average shear wave velocity between 360 m/s and 750 m/s. The third group consists of ground motions with average shear wave velocity between 180 m/s and 360 m/s. The last 40 ground motion records have average shear wave velocity lower than 180 m/s. All selected ground motions are given in Appendix, Table A1. Any other criterion was not considered for the selection of ground motions.

5 Analysis

The inelastic displacement ratio, C_R, is the ratio of maximum lateral inelastic displacement demand (u_i) to maximum lateral elastic displacement demand (u_e) of a SDOF system for *constant strength reduction factor* (R_y). It is expressed as

$$C_R = \frac{u_i}{u_e} \tag{3}$$

Strength reduction factor R_y is defined by:

$$R_y = f_e / f_y \tag{4}$$

In Eq. (4), f_e is the elastic strength of a corresponding linear system and f_y is the yield strength.

The inelastic displacement demand was computed for considered SDOF systems through nonlinear time history analysis. Newmark-Beta method was adopted in an in-house computer program for nonlinear time history analysis. SNAP [35] user guide was used for details of rules of cyclic degrading hysteretic model. Nonlinear time history analyses were conducted for SDOF systems having a viscous damping ratio of 5% with the following strength reduction factors R_y = 1.5, 2, 3, 4, 5, 6. The considered values of the post-yield stiffness ratio (α_s) are 0%, 3% and 5%, respectively. Inelastic displacement ratios were computed for a set of 53 natural vibration periods ranging from T = 0.1s. to T = 3s. (T = 0.1:0.02:0.2, 0.22:0.03:1, 1.1:0.1:3). 4273920 nonlinear time history analyses were performed to determine the inelastic displacement ratios with the 27 different combinations of degrading parameters and 1 non-degrading bilinear model.

6 Limit for Dynamic Instability (Collapse Period)

As mentioned in Section 3, collapse is considered with the hysteretic model used in this study based on two criteria: intersection of post-capping branch and horizontal axis (strength reaches zero) or exhausting of hysteretic energy dissipation capacity. The first condition is called “dynamic instability. In this study, the collapses were reached due to dynamic instability, in other words post-capping branch reaches the horizontal axis before hysteretic energy capacity is exhausted.

Chenouda and Ayoub [19] studied on the inelastic displacement ratio using the same hysteretic behaviour and the collapse assumption of this study and showed that the degrading systems with a period less than a certain one (limit period) collapse because of the dynamic instability. In other words, there is such limit period that a SDOF system which has shorter period than this limit period collapses because of dynamic instability. An example of inelastic displacement ratio plot is given in Fig. 5.

Table 2 Coefficient values for determination of T_{col} defined in Eq. (5) [36]

Site Class	Degradation Level	x_1	x_2	x_3	x_4	Correlation
	Severe	0.0760	1.9946	-2.1919	0.6819	0.99
A	Moderate	0.0500	2.0508	-1.6188	0.6950	0.99
	Low	0.0685	1.9516	-1.5128	0.8597	0.99
	Severe	0.1080	2.5910	-3.3714	1.4010	0.97
B	Moderate	0.0736	2.0795	-1.4281	1.2840	0.93
	Low	0.0520	1.9192	-1.6044	0.65463	0.98
	Severe	0.1127	1.9430	-3.3559	0.9167	0.96
C	Moderate	0.0660	1.6114	-1.7429	0.5218	0.97
	Low	0.0791	1.5530	-1.1348	0.8600	0.95
	Severe	0.0902	1.7420	-0.6007	0.6929	0.97
D	Moderate	0.1093	1.7232	-1.5604	0.5378	0.98
	Low	0.1735	1.6249	-1.9407	0.6922	0.96
	Severe	0.1123	2.0338	-2.7238	0.9330	0.98
All	Moderate	0.0873	1.7190	-1.4146	0.7963	0.98
	Low	0.0600	1.8424	-1.3995	0.6928	0.98

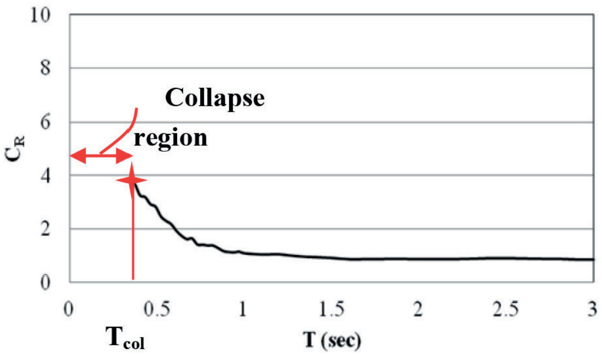

Fig. 5 An example for C_R plot considering collapse potential

The last point which is indicated with a "✦" in Fig. 5 is limit period for collapse and this limit period is called as "collapse period" (T_{col}). A system which has period shorter than the collapse period exhibits collapse because of dynamic instability and inelastic displacement demand cannot be determined for such a system. Thus, inelastic displacement ratio is not drawn in Fig. 5 for shorter periods than the collapse period. If the structure exhibits dynamic instability under the effect of more than 50% of the considered ground motion records then it is assumed that system with this period collapses [19].

An equation is proposed using the same hysteretic model for collapse period by Borekci et al. [36] as a function of the parameters considered in this study. Proposed equation of T_{col} is given in Eq. (5) and coefficients of Eq. (5) are given in Table 2. Detailed information for T_{col} can be seen in the study of Borekci et al. [36]

$$T_{col} = 0.1 + x_1 R^{x_2} \left(\left(\frac{u_c}{u_y} \right)^{x_3} + \alpha_C^{x_4} \right) \tag{5}$$

7 Mean Inelastic Displacement Ratio (C_R) for Bilinear Hysteretic Model

C_R of non-degrading bilinear hysteretic behaviour was also investigated to compare with that of degrading peak-oriented behaviour. In Fig. 6, mean C_R of all site classes using non-degrading bilinear hysteretic model were given for each considered post-yield stiffness ratio.

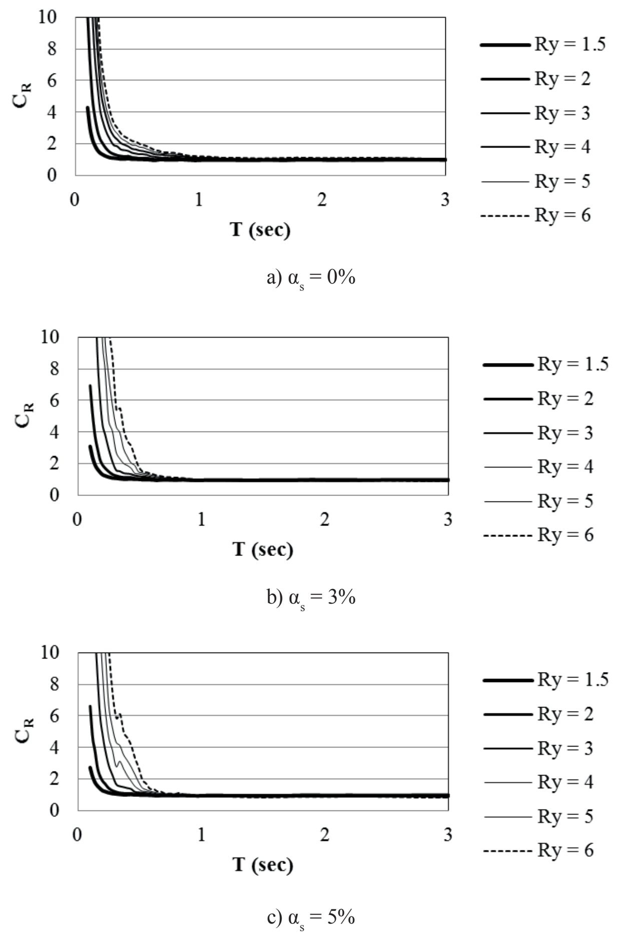

Fig. 6 Mean inelastic displacement ratios (C_R) for non-degrading bilinear hysteretic model

8 Mean Inelastic Displacement Ratio (C_R) for Peak-Oriented Hysteretic Model

8.1 Mean Ratios for All Site Classes

Mean inelastic displacement ratio (C_R) was computed for each period and each strength reduction factor using 27 different degradation cases. Plots of inelastic displacement ratio for different period values and different strength reduction factors were generated for all degradation cases. Plots of mean inelastic displacement ratio for 0% post-yield stiffness ratio (α_s = 0%) can be seen in Fig. 7 for different degradation cases.

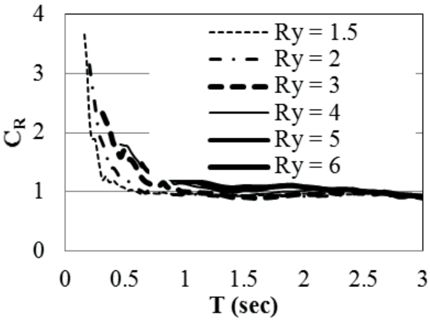

a) γ = 100, u_c/u_y = 4, α_c = -0.14

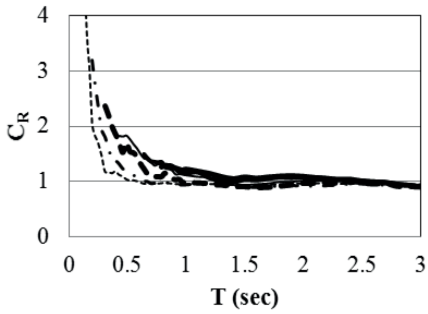

b) γ = 150, u_c/u_y = 4, α_c = -0.14

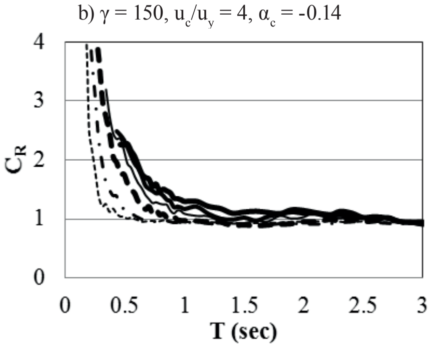

c) γ = 100, u_c/u_y = 6, α_c = -0.06

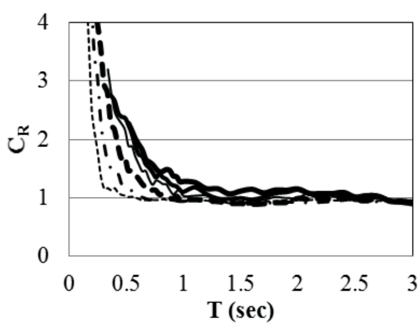

d) γ = 150, u_c/u_y = 6, α_c = -0.06

Fig. 7 C_R for degrading peak-oriented hysteretic model considering different degradation cases (α_s = 0%)

There is no inelastic displacement ratio for the periods shorter than T_{col} because of the collapse. Thus, initial period of each curve also shows T_{col}. It can be seen from Fig. 7 that mean C_R becomes approximately 1 for the period longer than a certain one (equal displacement rule) and beyond this period degradation is not effective on C_R. Note that this certain period is different for each degradation cases. However, for short period region, it is clear that degradation has apparent effects. Investigating the individual effect of each considered degradation parameter on the inelastic displacement ratio is not useful since degradation is a complex phenomenon and it is a result of the combination of those parameters. Thus, effect of degradation is investigated with the different combinations of the considered degradation parameters.

8.2 Effect of Local Site Conditions on C_R

Most of the current seismic design provisions ([37], [38], [39]) specify linear elastic design spectra based on different site classes. Thus, it is important to determine the effect of the local site conditions on inelastic displacement ratio to be used for estimating the maximum inelastic displacement from the maximum elastic displacement. Plots of inelastic displacement ratios for different local site conditions with the hysteretic parameters of γ = 100; u_c/u_y = 6; α_c = –0.06; α_s = 0 were given in Fig. 8. It is clear from Fig. 8 that local site conditions have significant effect on the inelastic displacement ratio, especially for site class D.

In Fig. 9, the ratio between mean $C_{R,ABCD}$ of all site classes and C_R obtained for each site class is shown. Each figure includes all the considered degradation parameter combinations and each point represents a different one. Fig. 9 was depicted for R_y =1.5 and 4, α_s = 0%. Fig. 9 is given to estimate the only general trend of effect of local site conditions on degradation cases since it is not easy to investigate the effect of local site conditions on each degradation cases individually. Thus, legend of Fig. 9 was not given.

According to Fig. 9, for R_y = 1.5, soil condition does not have effect on C_R for long period region (T > 0.7 sec), however it has significant effect on C_R for shorter periods. This result is valid for R_y= 2 also. It is clear form Fig. 9 that C_R for A, B and C site classes are generally lower than mean C_R of all site classes in the short period region while C_R for D site class is higher than mean C_R of all site classes for R_y= 4. In long period region, C_R for A, B and C site classes are close to mean C_R of all site classes for some degradation cases however it is not very close for some degradation cases. It can be said that generally C_R for A, B and C site classes are close to mean C_R of all site classes for most of degradation cases but not for all ones. R_y higher than 4 has same trend with this observation. Although, it is not easy to make an exact estimation for the effect of local site conditions on C_R for each degradation cases, it is clear that local site conditions must be considered in the estimation of mean inelastic displacement ratio.

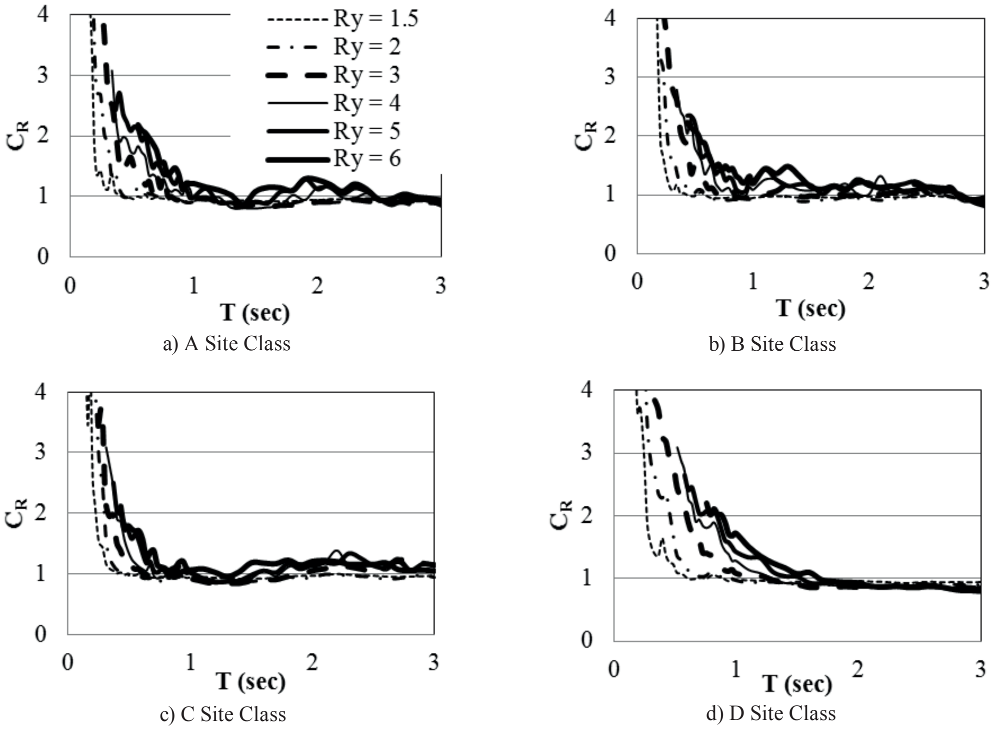

Fig. 8 Mean inelastic displacement ratios of peak-oriented hysteretic model for different local site conditions (γ = 100; u_c/u_y = 6; α_c = -0.06; α_s = 0)

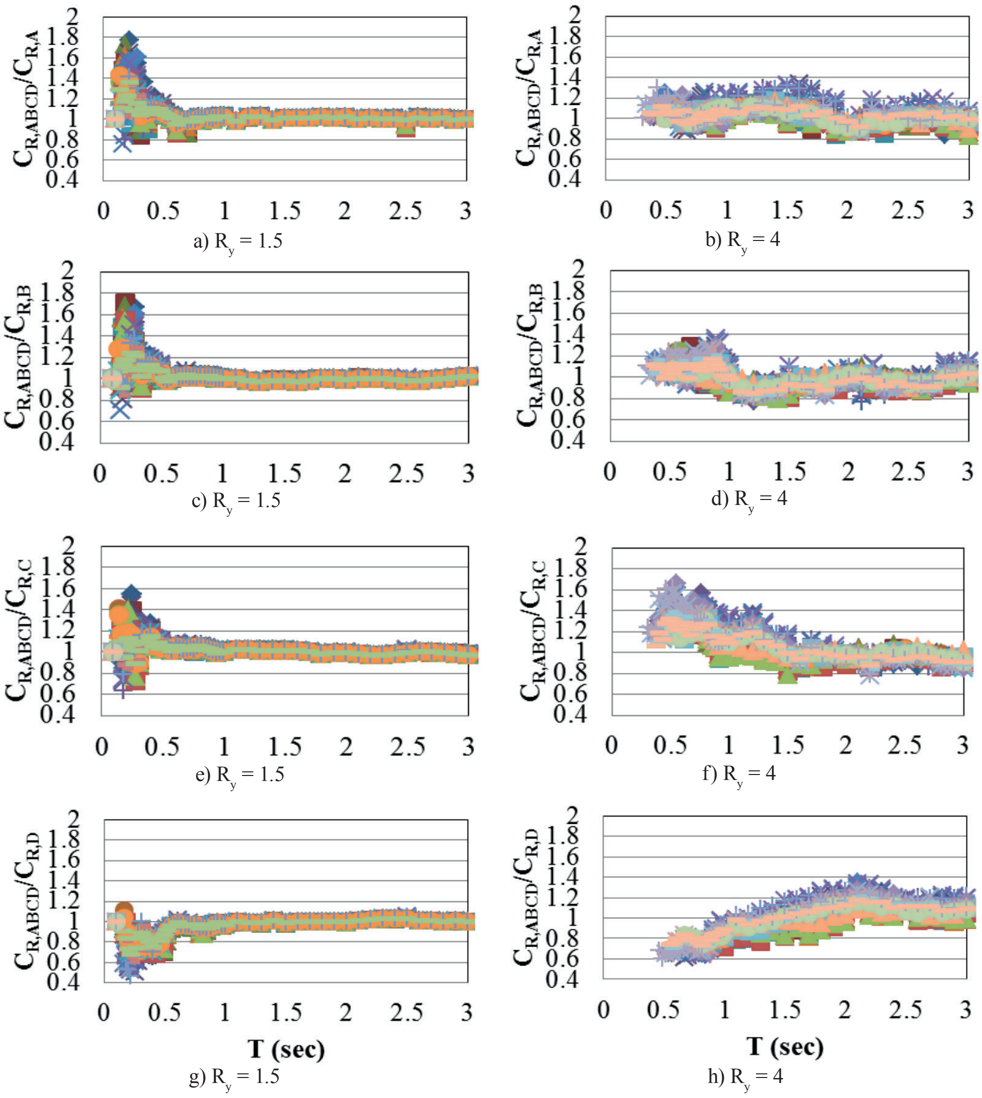

Fig. 9 Ratio of C_R for all site classes to C_R for each site class

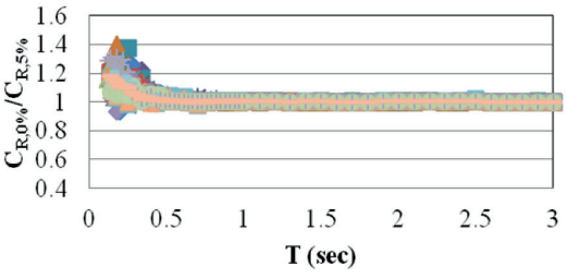

a) $R_y = 1.5$

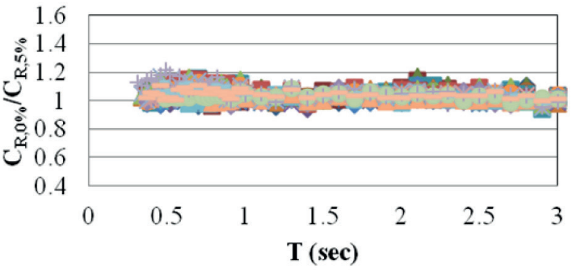

b) $R_y = 4$

Fig. 10 Ratios of C_R of $\alpha_s = 0\%$ to C_R of $\alpha_s = 5\%$ for degrading peak-oriented hysteretic model for two different R_y values

8.3 Effect of Post-Yield Stiffness on C_R

C_R with post-yield stiffness ratios of 0%, 3%, and 5% were computed to investigate the effect of the post-yield stiffness. Fig. 10 shows ratios of C_R with $\alpha_s = 0\%$ and $\alpha_s = 5\%$ including all degradation combinations for $R_y = 1.5$ and $R_y = 4$. It can be seen that C_R of $\alpha_s = 5\%$ is smaller than that of $\alpha_s = 0\%$, generally. But this ratio depends on the degradation parameter combinations. However, for long period regions C_R does not change with the post-yield stiffness.

9 Comparisons for Degrading and Non-degrading Hysteretic Models

In Fig. 11, C_R of bilinear and peak-oriented hysteretic models were given for $R_y = 2$ and 4 considering $\gamma = 50$, $u_c/u_y = 2$, $\alpha_c = -0.14$ and $\gamma = 150$, $u_c/u_y = 6$, $\alpha_c = -0.06$ degradation cases and $\alpha_s = 0\%$. It is clear from the figure that C_R of degrading systems is generally higher than that of bilinear system, especially for low periods.

C_R of bilinear hysteretic model and C_R of peak-oriented hysteretic model for all degradation cases were given in Fig. 12. Fig. 12 was depicted for $R_y = 3$ and 5, all site classes and $\alpha_s = 0\%$. In Fig. 12, the dashed line shows the mean C_R values of the non-degrading bilinear model. It is clear from Fig. 12 that degradation has considerable effect on C_R and bilinear hysteretic model estimates lower C_R values. Previous studies ([15], [16], [19], [20]) concluded the same result with the finding of this study.

Chenouda and Ayoub [19] stated that inelastic displacement demand of bilinear system is lower than that of peak-oriented hysteretic model also as stated in this study. Using unique non-degrading bilinear hysteretic model to determine C_R for building whose periods are same but ductility and strength levels are different is not conservative.

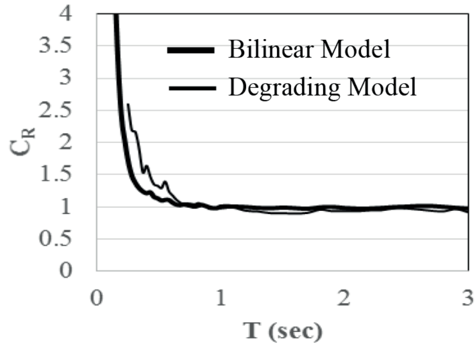

a) $R_y = 2$; $\gamma = 50$, $u_c/u_y = 2$, $\alpha_c = -0.14$

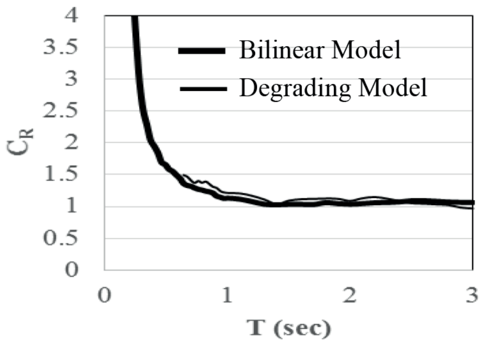

b) $R_y = 4$; $\gamma = 50$, $u_c/u_y = 2$, $\alpha_c = -0.14$

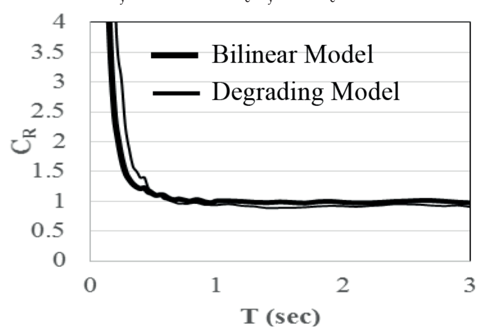

c) $R_y = 2$; $\gamma = 150$, $u_c/u_y = 6$, $\alpha_c = -0.06$

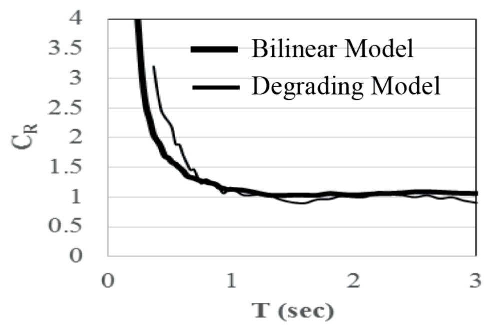

d) $R_y = 4$; $\gamma = 150$, $u_c/u_y = 6$, $\alpha_c = -0.06$

Fig. 11 Comparisons of C_R of non-degrading bilinear and degrading peak-oriented models

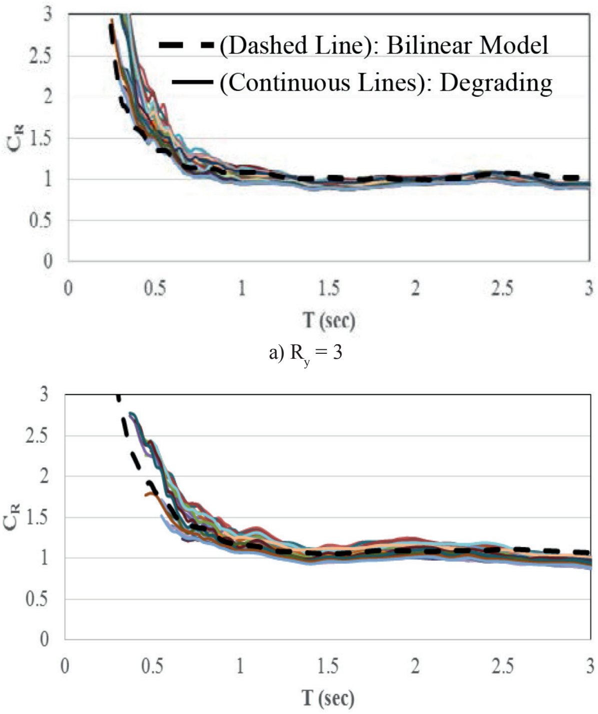

a) R_y = 3

b) R_y = 5

Fig. 12 C_R for all degradation cases and C_R for non-degrading bilinear hysteretic model

10 Nonlinear Regression Analysis

Nonlinear regression analyses were carried out to obtain an appropriate equation to represent the constant strength mean inelastic displacement ratio as a function of R_y, T, γ, u_c/u_y and α_c. Using the Levenberg-Marquardt method in the regression module of STATISTICA [40] nonlinear regression analyses were conducted to derive a simplified equation. The proposed equation is expressed as:

$$C_R = 1 + a\frac{(R-1)^b}{T^C}\left(\frac{\left(\frac{u_c}{u_y}\right)^d}{(\alpha_c)^e} + \left(\frac{1}{\gamma^f}\right)\right) \quad (6)$$

In Eq. (6), a, b, c, d, e, f are coefficients and summarized in Table 3 for different site classes individually and also considering all site classes. Fig. 13 shows the fitness of the Eq. (6) of the mean C_R. Also Fig. 14 shows the dispersion of the regressed function of C_R. In Fig. 14, horizontal axis shows the mean C_R obtained from nonlinear dynamic analyses and vertical axis shows C_R obtained with proposed equation. It is seen from Fig. 13 and Fig. 14 that proposed equation provides a good approximation of the mean inelastic displacement ratio. As mentioned in Section 6, Eq. (6) is valid on condition that the period of the system is longer than the collapse period ($T>T_{col}$).

11 Conclusions

It is clear from the previous studies that an RC building degrades and can reach collapse state under a severe cyclic lateral loading such as earthquake motions. Thus, in this study, constant lateral strength inelastic displacement ratio of SDOF systems which considers stiffness and strength degrading hysteretic behaviour with collapse potential were investigated for the period range 0.1 - 3 s. with different degradation levels using 160 ground motion records. For this purpose, an energy based degrading Modified-Clough hysteretic model with collapse potential was considered as the hysteretic behaviour. Inelastic displacement ratio of non-degrading bilinear hysteretic model were determined for the same data to investigate the effect of degradation and hysteretic model. A new equation was proposed for mean inelastic displacement ratio of degrading SDOF systems with collapse potential as a function of degradation parameters (γ, u_c/u_y, α_c), structural period (T) and strength reduction factor (R_y). The proposed equation for mean inelastic displacement ratio provides good fitting with the exact values of mean inelastic displacement ratio. Following conclusions can also be drawn from the results of this study:

- The inelastic displacement ratio is clearly affected by the local site conditions, where the ground motion is recorded, in case of degradation. Thus, the local site conditions must be considered in the estimation of mean inelastic displacement ratio of degrading SDOF systems.
- The post-yield stiffness ratio has an effect on mean inelastic displacement ratio for the short period systems whose R_y = 1.5 and 2. However, this effect becomes less significant with increasing R_y. Authors believe that it is not necessary to consider the post-yield stiffness ratio in the estimation of mean inelastic displacement ratio of degrading peak-oriented hysteretic model since the general effect of post-yield stiffness ratio on mean inelastic displacement ratio is not significant. Thus, it is efficient and conservative to use α_s = 0% for the engineering practice since the degrading system with α_s = 0% gives higher C_R at all cases.

Table 3 Coefficients of C_R defined in Eq. (6)

Site Class	a	b	c	d	e	f	Correlation coefficient
A	0.0078	0.9824T+0.8445	0.4013T+3.0625	-0.3214	0.4366	0.3324	0.94
B	0.0064	1.2892T+0.5428	0.7134T+2.9928	-0.3691	0.5305	0.2508	0.94
C	0.0003	1.0749T+0.5532	7.9249T+3.5381	-0.1897	0.4752	0.3200	0.95
D	0.0302	0.5372T+0.7244	1.5999T+2.1872	-0.1706	0.4454	0.2784	0.95
All	0.0115	0.7354T+0.7219	0.5749T+2.7944	-0.2765	0.4871	0.2732	0.97

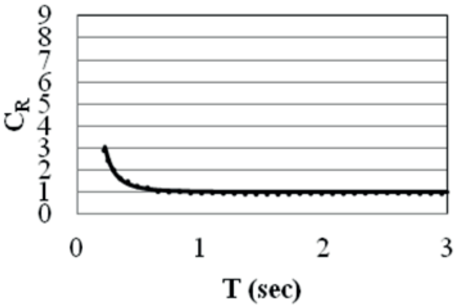

a) $R_y = 2$; $\gamma = 50$, $u_c/u_y = 4$, $\alpha_c = -0.14$

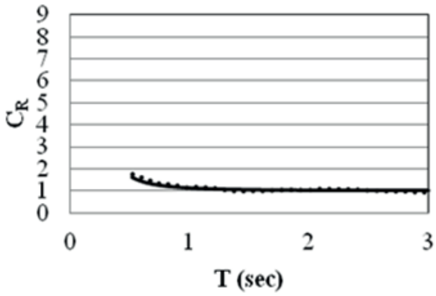

b) $R_y = 4$; $\gamma = 50$, $u_c/u_y = 4$, $\alpha_c = -0.14$

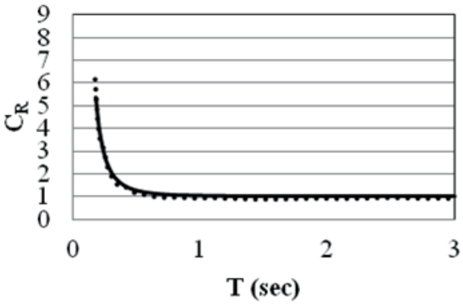

c) $R_y = 2$; $\gamma = 150$, $u_c/u_y = 6$, $\alpha_c = -0.06$

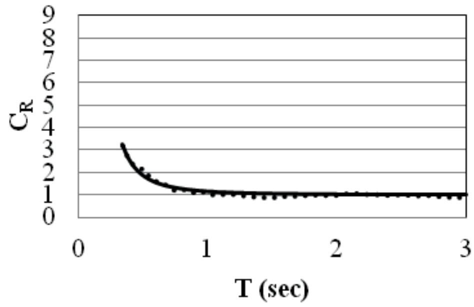

d) $R_y = 4$; $\gamma = 150$, $u_c/u_y = 6$, $\alpha_c = -0.06$

Fig. 13 Comparison of C_R obtained from nonlinear time history analyses and obtained with proposed equation

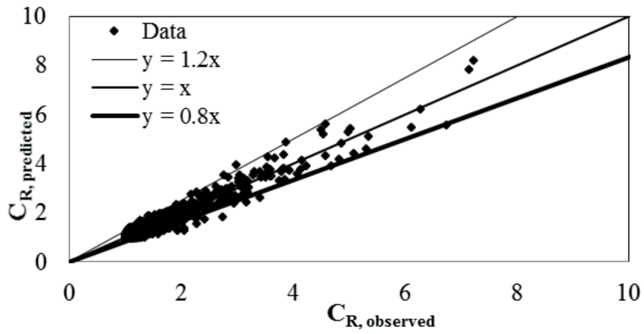

a) A Site Class

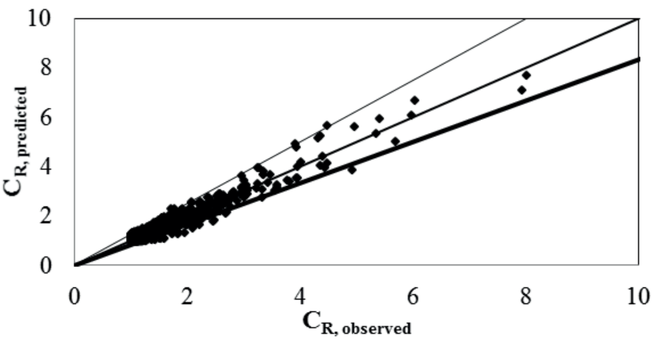

b) B Site Class

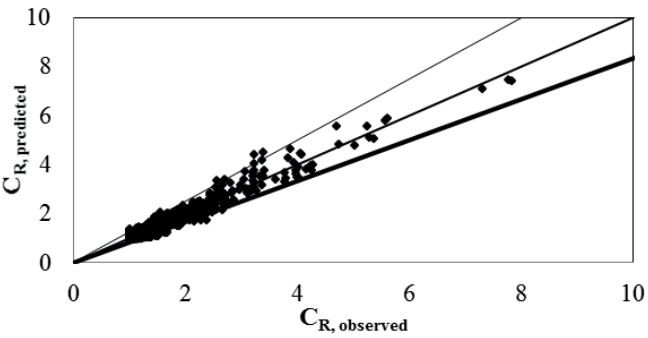

c) C Site Class

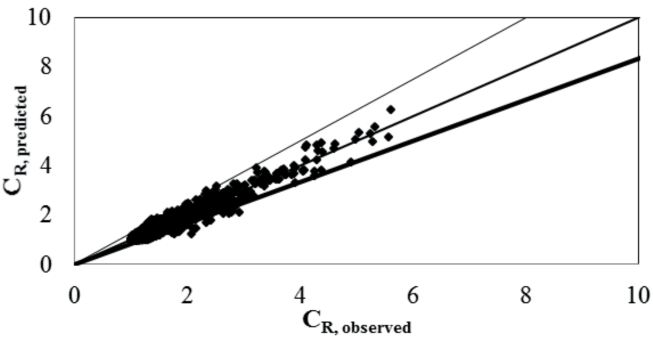

d) D Site Class

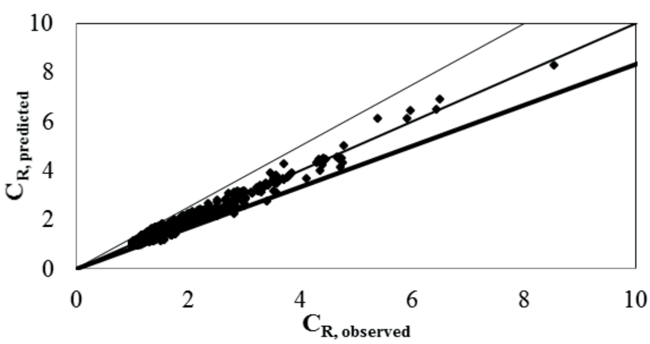

d) All Site Classes

Fig. 14 Dispersion of the proposed equation

- Non-degrading bilinear hysteretic model gives lower C_R than that of degrading peak-oriented hysteretic model.
- Using non-degrading bilinear hysteretic model for structures have same stiffness but different ductility, degradation and collapse potential is not conservative. Degrading peak-oriented hysteretic model realistically represents hysteretic behaviour of RC buildings, thus using a degrading model which considers different degradation cases is more realistic and conservative than using a non-degrading bilinear hysteretic model.
- The proposed equation has a good fit with the theoretical values and it is realistic and conservative in the estimation of C_R of RC buildings comparing to the non-degrading bilinear hysteretic model.
- According to Fig. 12, degradation has significant effect on C_R. Inelastic displacement demand is different for buildings which have different ductility and strength but same period. Thus, the proposed equation can be used for RC buildings with different degradation cases and levels.

References

[1] Veletsos, A. S., Newmark, N. M. "Effect of inelastic behavior on the response of simple systems to earthquake motions". In: *Proceedings of the 2nd World Conference on Earthqauke Engineering. 2,* Tokyo, Japan, pp. 895–912, 1960. http://www.iitk.ac.in/nicee/wcee/article/vol.2_session2_895.pdf

[2] Newmark, N. M., Hall, W. J. *Earthquake spectra and design*. Earthquake Engineering Research Institute, University of Illinois at Urbana-Champaign. 1982.

[3] Shimazaki, K., Sozen, M.A. "Seismic drift of reinforced concrete structures". *Research Report*, Hazama-Gumi Ltd., Tokyo, Japan, 1984.

[4] Qi, X., Moehle, J. P., "Displacement design approach for reinforced concrete structures subjected to earthquakes". *Report No: UCD/EERC 91/02*,EERC Berkeley, CA,USA, 1991.

[5] Miranda, E. "Seismic evaluation and upgrading of existing structures". Ph.D. Dissertation, Univ. of California at Berkeley, Berkeley, California, 1991.

[6] Miranda, E. "Evaluation of seismic design criteria for highway bridges". *Earthquake Spectra*, 9(2), pp. 233–250, 1993. https://doi.org/10.1193/1.1585714

[7] Miranda, E. "Evaluation of site-dependent inelastic seismic design spectra". *J. of Structural Eng., vol. 119, no. 5*, pp. 1319–1338, 1993. https://doi.org/10.1061/(ASCE)0733-9445(1993)119:5(1319)

[8] Miranda, E., "Inelastic displacement ratios for structures on firm sites". *Jornal of Structural Engineering,* 126(10), pp. 1150–1159. 2000. https://doi.org/10.1061/(ASCE)0733-9445(2000)126:10(1150)

[9] Ruiz-Garcia, J., Miranda, E. "Inealstic Displacement Ratios for Evaluation of Existing Structures". *Earthquake Engineering & Structural Dynamics,* 32(8), pp. 1237–1258. 2003. https://doi.org/10.1002/eqe.271

[10] Nassar, A. A., Krawinkler, H. "Seismic Demands for SDOF and MDOF Systems". *Report No. 95*, John A. Blume Earthquake Engineering Center, Stanford Univ., 1991.

[11] Rahnama, M., Krawinkler, H. "Effects of soft soil and hysteresis model on seismic demands". *Report No. 108*, John A. Blume Earthquake Engineering Center, Stanford Univ., 1993.

[12] Seneviratna, G. D. P. K., Krawinkler, H. "Evaluation of inelastic MDOF effects for seismic design". *Report No. 120*, John A. Blume Earthquake Engineering Center, Stanford Univ. 1997.

[13] Vidic, T., Fajfar, P., Fishinger, M. "Consistent inelastic design spectra: strength and displacement". *Earthquake Engineering & Structural Dynamics,* 23(5), pp. 507–528, 1994. https://doi.org/10.1002/eqe.4290230504

[14] Gupta, B., Kunnath, S. K. "Effect of Hysteretic Model Parameters on Inelastic Seismic Demands". *Proceedings of the 6th US National Conference on Earthqauke Engineering,* Seattle, Whashington. May 31–Jun. 04. 1998.

[15] Song, J.K., Pincheira, J. "Spectral displacement demands of stiffness-and strength-degrading systems". *Earthquake Spectra,* 16(4), pp. 817–851. 2000. https://doi.org/10.1193/1.1586141

[16] Pekoz, H. A., Pincheira, J. A. "Seismic Response of Strength and Stiffness Degrading Single Degree of Freedom Systems". *13th World Conference on Earthqauke Engineering,* Vancouver, Canada, Aug. 1–6. 2004. http://www.iitk.ac.in/nicee/wcee/article/13_936.pdf

[17] Aydinoglu, M. N., Kacmaz, U. "Strength-based displacement amplification spectra for inelastic seismic performance evaluation". *Report No. 2002/2*, Kandilli Observatory and Earthqauke Research Institute Department of Earthquake Engineering, Istanbul, Turkey, 2002.

[18] Chopra, A. K., Chintanapakdee, C."Inelastic Deformation Ratios for Design and Evaluation of Structures: Single-Degree-of-Freedom Bilinear Systems". *Journal of Structural Emgineering,* 130(9), pp. 1309–1319, 2004. https://doi.org/10.1061/(ASCE)0733-9445(2004)130:9(1309)

[19] Chenouda, M., Ayoub, A. "Inelastic Displacement Ratios of Degrading Systems". *Journal of Structural Engineering,* 134(6), pp. 1030–1045. 2008. DOI: https://doi.org/10.1061/(ASCE)0733-9445(2008)134:6(1030)

[20] Lumantarna, E., Lam, N., Wilson, J., Griffith, M."Inelastic Displacement Demand of Strength-Degraded Structures". *Journal of Earthquake Engineering,* 14(4), pp. 487–511. 2010. https://doi.org/10.1080/13632460903336910

[21] Eser, M., Aydemir, C., Ekiz, I. "Inelastic displacement ratios for structures with foundation flexibility". *KSCE Journal of Civil Engineering,* 16(1), pp. 155–162. 2012. https://doi.org/10.1007/s12205-012-1266-5

[22] Ibarra, L.F., Medina, R.A., Krawinkler, H. "Hysteretic models that incorporate strength and stiffness deterioration". *Earthquake Engineering Structural Dynamics,* 34(12), pp. 1489–1511, 2005. https://doi.org/10.1002/eqe.495

[23] Braz-Cesar, M. T., Oliveira, D., Barros, R.C. "Comparison of Cyclic Response of Reinforced Concrete Infilled Frames With Experimental Results". *Proceedings of 14th World Conference on Earthqauke Engineering,* Beijing China, Oct. 12–17. 2008. http://www.14wcee.org/Proceedings/files/05-03-0204.PDF

[24] Chintanapakdee, C., Jaiyong, A. "Estimation of Peak Roof Displacement of Degrading Structures". *Proceedings of 15th World Conference on Earthqauke Engineering,* Lisbon, Portugal, 2012. http://www.iitk.ac.in/nicee/wcee/article/WCEE2012_0835.pdf

[25] Otani, S. "Hysteresis Models of Reinforced Concrete for Earthquake Response Analysis". *Journal of the Faculty of Engineering,* 36(2), pp. 125–159. 1981.

[26] Clough, R., Johnston, S. B. "Effect of stiffness degradation on earthquake ductility requirements". *Transactions of Japan Earthquake Engineering Symposium,* Japan, 1966.

[27] Mahin, S. A., Bertero, V. V. "An evaluation of some methods for predicting seismic behavior of reinforced concrete buildings". *Report No. 75-5*, Earthquake Engineering Research Center, Univ. of California at Berkeley, 1975.

[28] FEMA P440A, "*Effects of strength and stiffness degradation on the seismic response*". Federal Emergemcy Management Agency, Washington DC, 2009. https://www.fema.gov/media-library-data/20130726-1719-25045-0771/fema_p440a.pdf

[29] Ibarra L.F., Krawinkler, H. "Global collapse of frame structures under seismic excitations". *Report No. 125*, John A. Blume Earthquake Engineering Center,Stanford Univ., 2005. http://peer.berkeley.edu/publications/peer_reports/reports_2005/PEER_506_IBARRA_krawinkler.pdf

[30] Miranda, E., Akkar, S. D., "Dynamic Instability of Simple Structural Systems". *Jourlnal of Structural Engineering,* 129(12), pp. 1722–1726, 2003. https://doi.org/10.1061/(ASCE)0733-9445(2003)129:12(1722)

[31] Bernal, D. "Instability of buildings during seismic response". *Engineering Strucures,* 20(4–6), pp. 496–502. 1998. https://doi.org/10.1016/S0141-0296(97)00037-0

[32] Villaverde, R., "Methods to Assess the Seismic Collapse Capacity of Building Structures: State of the Art". *Journal of Structural Engineering,* 133(1), pp. 57–66, 2007. https://doi.org/10.1061/(ASCE)0733-9445(2007)133:1(57)

[33] Ayoub, A., Chenouda, M. "Response spectra of degrading structural systems". *Engineering Structures,* 31(7), pp. 1393–1402. 2009. https://doi.org/10.1016/j.engstruct.2009.02.006

[34] USGS, U.S. Geological Survey. http://www.usgs.gov/

[35] Ibarra, L.F. "SNAP Program User Guide". 2002.

[36] Borekci, M., Kirçil, M. S., Ekiz, I. "Collapse period of degrading SDOF systems". *Earthquake Engineering and Engineering Vibration,* 13(4), pp. 681–694, 2014. https://doi.org/10.1007/s11803-014-0272-7

[37] FEMA 356, *Prestandard and Commentary for the Seismic Rehabilitation of Buildings*, Federal Emergemcy Management Agency, Washington DC, 2000. http://sharif.edu/~ahmadizadeh/courses/strcontrol/CIE626-2-FEMA-356.pdf

[38] TSC 2007, Turkish Seismic Code, Ankara, Turkey, 2007.

[39] ATC 40, *Seismic Evaluation and Retrofit of Concrete Buildings*, Applied Technology Council, 1996. http://www.dinochen.com/attachments/month_0901/atc-402.pdf

[40] STATISTICA. http://www.statsoft.com StatSoft Inc.

Appendix

Table A1 Considered ground motion records

NGA#	Event	Year	Station	Mag	R_{rup} (km)	Soil Class
59	San Fernando	1971	Cedar Springs, Allen Ranch	6.61	89.7	A
788	Loma Prieta	1989	Piedmont Jr High	6.93	73	A
789	Loma Prieta	1989	Point Bonita	6.93	83.5	A
795	Loma Prieta	1989	SF - Pacific Heights	6.93	76	A
797	Loma Prieta	1989	SF - Rincon Hill	6.93	74.1	A
804	Loma Prieta	1989	So. San Francisco, Sierra Pt.	6.93	63.1	A
925	Big Bear-01	1992	Rancho Cucamonga - Deer Can	6.46	59.4	A
943	Northridge-01	1994	Anacapa Island	6.69	68.9	A
946	Northridge-01	1994	Antelope Buttes	6.69	46.9	A
1033	Northridge-01	1994	Littlerock - Brainard Can	6.69	46.6	A
1041	Northridge-01	1994	Mt Wilson - CIT Seis Sta	6.69	35.9	A
1060	Northridge-01	1994	Rancho Cucamonga - Deer Can	6.69	80	A
1074	Northridge-01	1994	Sandberg - Bald Mtn	6.69	41.6	A
1096	Northridge-01	1994	Wrightwood - Jackson Flat	6.69	64.7	A
1518	Chi-Chi, Taiwan	1999	TCOLU085	7.62	58.1	A
2633	Chi-Chi, Taiwan-03	1999	TCOLU085	6.2	103.6	A
2687	Chi-Chi, Taiwan-03	1999	TTN042	6.2	93.5	A
2805	Chi-Chi, Taiwan-04	1999	KAU003	6.2	116.2	A
2929	Chi-Chi, Taiwan-04	1999	TTN042	6.2	69	A
2996	Chi-Chi, Taiwan-05	1999	HWA003	6.2	50.4	A
56	San Fernando	1971	Carbon Canyon Dam	6.61	61.8	B
58	San Fernando	1971	Cedar Springs Pumphouse	6.61	92.6	B
63	San Fernando	1971	Fairmont Dam	6.61	30.2	B
83	San Fernando	1971	Puddingstone Dam (Abutment)	6.61	52.6	B
86	San Fernando	1971	San Onofre - So Cal Edison	6.61	124.8	B
89	San Fernando	1971	Tehachapi Pump	6.61	63.8	B
91	San Fernando	1971	Upland - San Antonio Dam	6.61	61.7	B
94	San Fernando	1971	Wrightwood - 6074 Park Dr	6.61	62.2	B
121	Friuli, Italy-01	1976	Barcis	6.5	49.4	B
124	Friuli, Italy-01	1976	Feltre	6.5	102.2	B
323	Coalinga-01	1983	Parkfield - Cholame 12W	6.36	55.8	B
325	Coalinga-01	1983	Parkfield - Cholame 2E	6.36	42.9	B
327	Coalinga-01	1983	Parkfield - Cholame 3E	6.36	41	B
330	Coalinga-01	1983	Parkfield - Cholame 4W	6.36	46.4	B
1154	Kocaeli, Turkey	1999	Bursa Sivil	7.51	65.5	B
1159	Kocaeli, Turkey	1999	Eregli	7.51	142.3	B
1162	Kocaeli, Turkey	1999	Goynuk	7.51	31.7	B
1163	Kocaeli, Turkey	1999	Hava Alani	7.51	60	B
1164	Kocaeli, Turkey	1999	Istanbul	7.51	52	B
1172	Kocaeli, Turkey	1999	Tekirdag	7.51	165	B
52	San Fernando	1971	Anza Post Office	6.61	173.2	C
54	San Fernando	1971	Borrego Springs Fire Sta	6.61	214.3	C
62	San Fernando	1971	Colton - So Cal Edison	6.61	96.8	C
66	San Fernando	1971	Hemet Fire Station	6.61	139.1	C
85	San Fernando	1971	San Juan Capistrano	6.61	108	C
122	Friuli, Italy-01	1976	Codroipo	6.5	33.4	C
123	Friuli, Italy-01	1976	Conegliano	6.5	80.4	C
166	Imperial Valley-06	1979	Coachella Canal #4	6.53	50.1	C

NGA#	Event	Year	Station	Mag	R_{rup} (km)	Soil Class
188	Imperial Valley-06	1979	Plaster City	6.53	30.3	C
268	Victoria, Mexico	1980	SAHOP Casa Flores	6.33	39.3	C
324	Coalinga-01	1983	Parkfield - Cholame 1E	6.36	43.7	C
326	Coalinga-01	1983	Parkfield - Cholame 2WA	6.36	44.7	C
328	Coalinga-01	1983	Parkfield - Cholame 3W	6.36	45.7	C
329	Coalinga-01	1983	Parkfield - Cholame 4AW	6.36	47.6	C
331	Coalinga-01	1983	Parkfield - Cholame 5W	6.36	48.7	C
1149	Kocaeli, Turkey	1999	Atakoy	7.51	58.3	C
1153	Kocaeli, Turkey	1999	Botas	7.51	127	C
1157	Kocaeli, Turkey	1999	Cekmece	7.51	66.7	C
1160	Kocaeli, Turkey	1999	Fatih	7.51	55.5	C
452	Morgan Hill	1984	Foster City - APEEL 1	6.19	53.9	D
732	Loma Prieta	1989	APEEL 2 - Redwood City	6.93	43.2	D
759	Loma Prieta	1989	Foster City - APEEL 1	6.93	43.9	D
760	Loma Prieta	1989	Foster City - Menhaden Court	6.93	45.6	D
780	Loma Prieta	1989	Larkspur Ferry Terminal (FF)	6.93	94.6	D
808	Loma Prieta	1989	Treasure Island	6.93	77.4	D
962	Northridge-01	1994	Carson - Water St	6.69	49.8	D
1147	Kocaeli, Turkey	1999	Ambarli	7.51	69.6	D
1229	Chi-Chi, Taiwan	1999	CHY078	7.62	77.2	D
1357	Chi-Chi, Taiwan	1999	KAU011	7.62	101.8	D
1599	Duzce, Turkey	1999	Ambarli	7.14	188.7	D
2493	Chi-Chi, Taiwan-03	1999	CHY078	6.2	98.6	D
2561	Chi-Chi, Taiwan-03	1999	ILA044	6.2	125.5	D
2718	Chi-Chi, Taiwan-04	1999	CHY054	6.2	61.1	D
2736	Chi-Chi, Taiwan-04	1999	CHY076	6.2	56.4	D
2737	Chi-Chi, Taiwan-04	1999	CHY078	6.2	84	D
2818	Chi-Chi, Taiwan-04	1999	KAU045	6.2	119.2	D
2958	Chi-Chi, Taiwan-05	1999	CHY054	6.2	92.3	D
2975	Chi-Chi, Taiwan-05	1999	CHY076	6.2	87.6	D
2976	Chi-Chi, Taiwan-05	1999	CHY078	6.2	116.4	D